DIFFUSION IN LIPID BILAYERS CONTAINING BARRIERS

A. A. RIGOS, DANIEL F. CALEF, AND J. M. DEUTCH
Department of Chemistry, Massachusetts Institute of Technology, Cambridge, Massachusetts 02139

ABSTRACT In epithelial cells, a barrier or tight junction restricts the diffusion of lipid probes from the apical to the basolateral side of the outer membrane bilayer. This phenomenon is studied theoretically with the diffusion equation on planar and spherical surfaces. Two models for the tight junction are considered: a penetrable barrier embedded in a monolayer and an impenetrable obstacle in the outer membrane of a bilayer that must be bypassed by flip-flopping between inner and outer membranes. The rate of passing from one side of the cell to the other is calculated for each of these models under steady state conditions. The results are compared with recent fluorescent photobleaching recovery experiments. The theoretical interpretation indicates that it would be difficult to distinguish experimentally between the flip-flop case and the barrier crossing case. Assuming a flip-flop model, large differences in the magnitude of the flip-flop rates of probes are necessary to explain the experimental results as suggested by Dragsten et al. (Dragsten, P. R., R. Blumenthal, and J. S. Handler, 1981, *Nature [Lond.]*, 294:718–722).

INTRODUCTION

There is considerable experimental evidence that the translational and rotational motion of probe molecules in biological membranes (1) is diffusional in character. The translational motion of the molecules can be modeled mathematically by the diffusion equation on a surface. Aizenbud and Gershon (2) studied the diffusion of molecules on membranes of nonplanar wavy form. Sano and Tachiya (3) modeled diffusion controlled reactions on micellar surfaces by examining the pair survival probability of two reacting particles on a spherical surface. Recent experimental work (4, 5) has explored the role and nature of the tight junction in the membrane of epithelial cells. It has been suggested (6, 7, 8, 9, 10) that the tight junction acts as an obstacle to the diffusion of certain membrane constituents between the apical and basolateral surfaces of individual cells.

Kachar and Reese (5) have evidence based on direct rapid freezing of newly formed tight junctions between rat prostate epithelial cells that suggests that individual tight junction strands are pairs of "inverted cylindrical micelles sandwiched between linear fusions of the external membrane leaflets of adjacent cells" (see Fig. 1 *a*). In the experiments of Dragsten and co-workers (4) one side of an epithelial monolayer of cells is labeled with a fluorescent lipid probe and the presence or absence of the fluorescent probe is observed on the opposite side of the monolayer. The rate of lateral diffusion of the probe is measured on both sides of the monolayer using the technique of fluorescence photobleaching recovery (FPR). Dragsten et al. (4) find that all the lipid probes are freely mobile on both the apical and basolateral membrane bilayers. Those that are able to spread over the entire cell in a few minutes have lateral diffusion coefficients ($D \sim 10^{-8}$ cm^2/s) at least twofold greater than those that can not traverse the cell ($D \sim 2 \times 10^{-9}$ cm^2/s). They also find a correlation between probes that can flip-flop between the two sides of the bilayer and those that can traverse the cell. The rates of flip-flopping of the lipid probes from outer to inner membrane and vice versa have not been measured by Dragsten et al. (4) and are not known for this system.

The purpose of this work is to model this diffusion process on a plane, and more realistically on a spherical surface. We develop two models for the tight junction aspect of the problem. In the first model, an impenetrable obstacle is placed on the outer leaf of the bilayer. Probes may only pass between the two halves of the cell by flipping to the inner leaf and flipping out again. This model is discussed in the following sections: Diffusion on a Planar Bilayer and Diffusion on a Spherical Bilayer.

The second model consists of a single, divided monolayer. The tight junction region is then treated as either a potential energy barrier, or as a region where the probe molecules have a much lower diffusion coefficient. This model is discussed in the Diffusion on a Monolayer with a Penetrable Barrier section. We assume that the membranes are a smooth surface and do not have microvilli. In each case, we calculate an analytic expression for the steady state rate coefficient. In the Results section we compare the results for the two models with available experiments.

Diffusion on a Planar Bilayer

In this section we formulate the model mathematically on a plane using a one-dimensional diffusion equation with appropriate boundary conditions. The concentrations of the lipid probes in the outer membrane, M1, and the inner membrane, M2, are denoted c_1 and c_2, respectively. For simplicity, we assume the same diffusion coefficient, D, for

the lipid probe in M1 and M2; likewise we assume the same flip-flop rate, λ, for flip-flopping of the lipid probe from M1 to M2 and vice versa. The model is depicted schematically in Fig. 1 *b*.

The tight junction or obstacle is a reflecting wall at $x = 0$ on M1. This makes it necessary to define the concentration c_1^+ on the interval x from 0 to $+l$, and c_1^- on the interval x from $-l$ to 0. The same definition is introduced for c_2. For steady state conditions, the concentrations c_1 and c_2 obey the coupled equations

$$D\nabla^2 c_1^\alpha - \lambda(c_1^\alpha - c_2^\alpha) = 0$$
$$D\nabla^2 c_2^\alpha + \lambda(c_1^\alpha - c_2^\alpha) = 0 \qquad (1)$$

where

$$\alpha = -, +, \nabla^2 = \frac{d^2}{dx^2}.$$

At $x = -l$ of M1, we have a source; c_1^- $(x = -l)$ is maintained at c_0. However at $x = +l$ of M1, we have a perfectly absorbing sink; c_1^+ $(x = +l)$ is maintained at 0. The inner membrane M2 plays its key role near $x = 0$; for M2 both $x = -l$ and $x = +l$ are perfectly reflecting walls. In summary, the boundary conditions are

$$c_1^- = c_0 \quad \text{at} \quad x = -l \qquad (2)$$

$$c_1^+ = 0 \quad \text{at} \quad x = +l \qquad (3)$$

$$\left.\frac{\partial c_2^+}{\partial x}\right|_{x=+l} = 0 \qquad (4)$$

$$\left.\frac{\partial c_2^-}{\partial x}\right|_{x=-l} = 0 \qquad (5)$$

$$\left.\frac{\partial c_1^+}{\partial x}\right|_{x=0} = 0 \qquad (6)$$

$$\left.\frac{\partial c_1^-}{\partial x}\right|_{x=0} = 0 \qquad (7)$$

$$c_2^+ = c_2^- \quad \text{at} \quad x = 0 \qquad (8)$$

$$\frac{\partial c_2^+}{\partial x} = \frac{\partial c_2^-}{\partial x} \quad \text{at} \quad x = 0. \qquad (9)$$

The boundary condition, Eqs. 8 and 9, which state continuity of the concentration and flux across M2 at $x = 0$, result from the absence of an obstacle on M2. In sum, the model requires molecules to proceed from the left side of M1 to absorption on the right side of M1 by a flip-flop movement to M2 to avoid the obstacle on M1 at $x = 0$. The solution of Eq. 1 with the boundary conditions in Eqs. 2–9 will yield the quantity of interest that is the flux on M1 at $x = +l$. The flux, J_{P1}, is found to be

$$J_{P1} = D\left.\frac{\partial c_1^+}{\partial x}\right|_{x=+l} = \frac{-Dc_0}{l + \dfrac{2(2+e^{\gamma l}+e^{-\gamma l})}{\gamma(e^{\gamma l}-e^{-\gamma l})}} \qquad (10)$$

where $\gamma^2 = 2\lambda/D$.

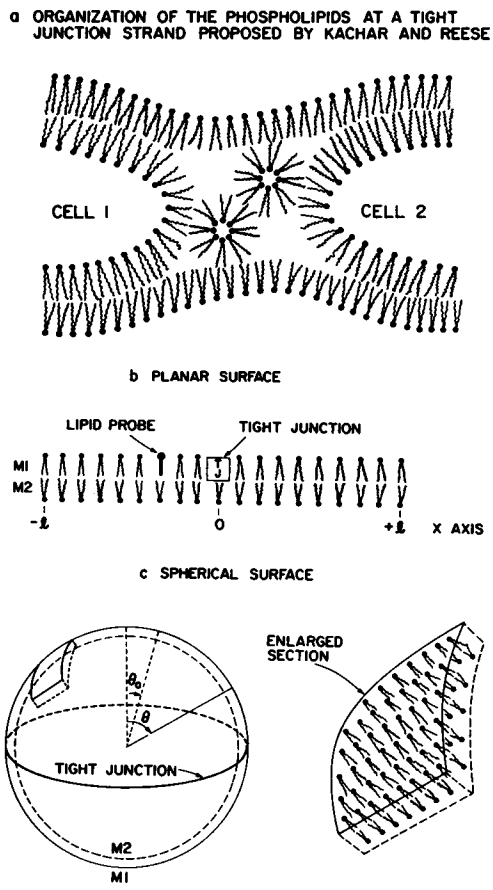

FIGURE 1 (*a*) Organization of the phospholipids at a tight junction strand proposed by Kachar and Reese (1982). (*b*) Planar model for tight junction in epithelial membrane bilayer: the obstacle at $x = 0$ separates the two halves of the outer leaf. (*c*) Spherical surface model for tight junction in epithelial membrane bilayer: the obstacle at $x = \cos(\pi/2) = 0$ separates the two halves of the outer leaf.

In the limit of no obstacle, the distinction between c_1^+ and c_1^- is no longer necessary and the boundary condition Eqs. 6–9 may be ignored. For this limiting case, the flux J_{P1} on M1 at $x = +l$ becomes

$$J_{P0} = \frac{-Dc_0}{l + \dfrac{e^{\gamma l} - e^{-\gamma l}}{\gamma(e^{\gamma l} + e^{-\gamma l})}}. \qquad (11)$$

As expected both J_{P0} and J_{P1} reduce to $J_{P\,monolayer} = -Dc_0/l$ as $\gamma \to \infty$, which means rapid flip-flopping. On the other hand, as $\gamma \to 0$, no flip-flopping, $J_{P0} \to J_{P\,monolayer}$ but $J_{P1} \to 0$ since without flip-flopping the obstacle prevents any flux of lipid probe.

Diffusion on a Spherical Bilayer

The problem of diffusion on a spherical bilayer is very similar to the problem addressed in the previous section except that in Eq. 1

$$\nabla^2 = \frac{1}{r^2 \sin\theta}\frac{\partial}{\partial\theta}\left(\sin\theta\frac{\partial}{\partial\theta}\right)$$

and

$$\alpha = + \quad \text{for} \quad \theta_0 < \theta < \frac{\pi}{2}$$

$$\alpha = - \quad \text{for} \quad \pi - \theta_0 > \theta > \frac{\pi}{2}. \tag{12}$$

The boundary conditions on the outer membrane, M1, of the spherical cell are such that a patch near the south pole ($\pi - \theta_0 < \theta < \pi$) is a source, at concentration of lipid probe c_0, while a patch near the north pole ($0 < \theta < \theta_0$) is a perfectly absorbing sink; the tight junction is a reflecting wall at the equator (see Fig. 1 *c*). For the inner membrane, M2, there are reflecting walls at both north and south pole patches. The boundary conditions are therefore identical to those for a planar bilayer, where l is replaced by $\cos\theta_0$ and generally $x = \cos\theta$. For simplicity the size of the source and sink polar patches were assumed equal and the reflecting obstacle on M1 was located at the equator rather than some general latitude. The solution of Eq. 1 with the modifications of Eq. 12 (see Appendix A) include the Legendre functions $P_\nu(x)$ and $Q_\nu(x)$, where $x = \cos\theta$, and their derivatives where

$$\nu = -\frac{1}{2} \pm [1 - 4\gamma^2 r^2]^{1/2}. \tag{13}$$

The flux across the tight junction is then

$$J_{S1} = D\frac{\partial c_2}{\partial x}\bigg|_{x=0} = -2Dc_0 P\prime(0) \cdot \left\{ \frac{[\pi^+ + M]}{\psi^+}[Q'_0(x_0)P'_\nu(0) + P'_\nu(x_0)] - \frac{[\pi^- + M]}{\psi^-}[Q'_0(x_0)P'_\nu(0) + P'_\nu(-x_0)] + P_\nu(-x_0) - P_\nu(x_0) + 2Q_0(x_0)P'_\nu(0) \right\}^{-1}, \tag{14}$$

where

$$x_0 = \cos\theta_0$$
$$\psi^+ = Q'_\nu(x_0)P'_\nu(0) - Q'_\nu(0)P'_\nu(x_0)$$
$$\psi^- = Q'_\nu(-x_0)P'_\nu(0) - Q'_\nu(0)P'_\nu(-x_0)$$
$$M = Q_\nu(0)P'_\nu(0) - P_\nu(0)Q'_\nu(0)$$
$$\pi^+ = Q_\nu(x_0)P'_\nu(0) - Q'_\nu(0)P_\nu(x_0)$$
$$\pi^- = Q_\nu(-x_0)P'_\nu(0) - Q'_\nu(0)P_\nu(-x_0).$$

For the case of no obstacle at the equator, the flux J_{S1} becomes (boundary condition Eqs. 6–9 can be ignored)

$$J_{S0} = \frac{2c_0 D}{\dfrac{Q'_0(x_0)[q'p - p'q]}{Q'_\nu(x_0)p' - q'P'_\nu(x_0)} - 2Q_0(x_0)} \tag{15}$$

where

$$x_0 = \cos\theta_0$$
$$q' = Q'_\nu(x_0) - Q'_\nu(-x_0)$$
$$p' = P'_\nu(x_0) - P'_\nu(-x_0)$$
$$p = P_\nu(x_0) - P_\nu(-x_0)$$
$$q = Q_\nu(x_0) - Q_\nu(-x_0)$$

for a spherical monolayer, the flux $J_{S\,\text{monolayer}}$ is simply

$$J_{S\,\text{monolayer}} = \frac{-Dc_0}{2Q_0(x_0)} \tag{16}$$

where

$$Q_0 = \frac{1}{2}\ln\frac{(1+x)}{(1-x)}.$$

The Legendre functions, P_ν and Q_ν, appearing in Eqs. 14 and 15 must be evaluated numerically. For small values of $\gamma^2 r^2$, perturbation expansions around $\nu = 0$ can be used, as in Tachiya and Sano (3). For larger values of $\gamma^2 r^2$, we calculate $P_\nu(x_0)$, $P'_\nu(x_0)$, $Q_\nu(x_0)$ and $Q'_\nu(x_0)$ by direct integration of Legendre's equation with the correct boundary conditions at $x = 0$, as given in Abramowitz and Stegun (13). For large values of $\gamma^2 r^2$, ν becomes a complex number of the form $\nu = 1/2 + i\tau$, and the relevant functions are the conical functions. For extremely large values of $\gamma^2 r^2$, asymptotic expressions for these functions, which can be found in Lebedev (15), were used.

Diffusion on a Monolayer with a Penetrable Barrier

The second model we consider for epithelial cells consists of diffusion on a monolayer separated into two halves by a penetrable barrier. The barrier can be modeled as either a potential energy barrier or as a region where the diffusing molecules have a much smaller diffusion coefficient, which slows their crossing. The two cases have similar mathematical formulations. Restricting ourselves to the planar case initially, diffusion in the presence of a potential can be described with the Smoluchowski diffusion equation,

$$\frac{\partial c}{\partial t} = D\frac{\partial^2 c}{\partial x^2} + D\frac{\partial}{\partial x}\left[c\frac{\partial \beta\phi(x)}{\partial x}\right], \tag{17}$$

where the potential energy of a particle at point x is $\phi(x)$ and $\beta = 1/K_B T$ (11). For the case in which the diffusion coefficient varies in space, the relevant equation is

$$\frac{\partial c}{\partial t} = \frac{\partial}{\partial x}\left[D(x)\frac{\partial c}{\partial x}\right]. \tag{18}$$

The calculation of the steady state flux, corresponding to that presented in previous sections, for Eqs. 17 and 18, was one of the classical contributions of Kramers (12). With

the boundary conditions

$$c = c_0 \quad \text{at} \quad x = -l$$
$$c = 0 \quad \text{at} \quad x = +l \tag{19}$$

the steady state flux corresponding to Eq. 17 is

$$J_{\text{PBAR}} = Dc_0 \left[\int_{-l}^{l} e^{\beta\phi(x)}\, dx \right]^{-1} \tag{20}$$

where we have assumed the potential vanishes sufficiently rapidly away from the origin. The flux corresponding (12) to Eq. 18 is

$$J_{\text{PDV}} = c_0 \left[\int_{-l}^{l} \frac{1}{D(x)}\, dx \right]^{-1} \tag{21}$$

To use these expressions we must assume a specific model for the tight junction. For the barrier case, the simplest reasonable model is to consider a strip near $x = 0$, from $-\epsilon$ to $+\epsilon$ where the potential $\phi(x)$ is a positive constant. The flux is then given by

$$J_{\text{PBAR}} = Dc_0 \left[2l + 2\epsilon \left(e^{\beta\phi} - 1\right)\right]^{-1}. \tag{22}$$

For the variable diffusion coefficient case, the corresponding model would be a strip near $x = 0$ where the diffusion coefficient D' is smaller than D. The resulting flux is

$$J_{\text{PDV}} = Dc_0 \left[2l + 2\epsilon \left(\frac{D}{D'} - 1\right)\right]^{-1} \tag{23}$$

The Eqs. 22 and 23 are identical in form with the identification

$$\beta\phi = \ln\left(\frac{D}{D'}\right), \tag{24}$$

and hence there is no operational difference between the two expressions in measurement of the steady state rate.

There is no difficulty in formulating this problem for a spherical surface of radius r. The appropriate diffusion equation is

$$\frac{\partial}{\partial x} D(1 - x^2) \left[\frac{\partial c}{\partial x} + c \frac{\partial \beta\phi(x)}{\partial x}\right] = 0, \tag{25}$$

where $x = \cos\theta$. The associated boundary conditions are a uniform source at the lower polar cap $c(-x_0) = c_0$ and a sink at the upper polar cap $c(+x_0) = 0$. For the case of variable diffusion coefficient $D = D(x)$ and no potential one obtains the steady state flux J_{DV} by direct integration

$$J_{\text{SDV}} = Dc_0 \left\{ \int_{-x_0}^{x_0} dx \left[\frac{D(x)}{D} (1 - x^2)\right]^{-1} \right\}^{-1}. \tag{26}$$

The limiting case of uniform diffusion coefficient yields

$$J^0_{\text{SDV}} = -Dc_0 \left[2\, Q_0(x_0)\right]^{-1}, \tag{27}$$

where the function $Q_0(x)$ is defined (13) by

$$Q_0(x) = \frac{1}{2} \ln\left(\frac{1 + x}{1 - x}\right).$$

The special case where a small strip of width 2ϵ astride the equator has diffusion coefficient D' yields the flux

$$J^{\epsilon}_{\text{SDV}} = Dc_0 \left\{2Q_0(x_0) + 2Q_0(\epsilon) \left[\frac{D}{D'} - 1\right]\right\}^{-1} \tag{28}$$

For the case of diffusion on a spherical surface in a potential $\phi(x)$ that acts as a barrier one finds

$$J_{\text{SBAR}} = Dc_0 \exp\left[\beta\phi(x_0)\right] \cdot \left\{ \int_{-x_0}^{x_0} dx \exp\left[\beta\phi(x)\right](1 - x^2)^{-1} \right\}^{-1} \tag{29}$$

The special case, where a small strip of width ϵ at the equator has a nonzero constant potential, ϕ, yields the result

$$J^{\epsilon}_{\text{SBAR}} = Dc_0 \left\{2Q_0(x_0) + 2Q_0(\epsilon) \left[e^{\beta\phi} - 1\right]\right\}^{-1}. \tag{30}$$

The results, Eqs. 26 and 29, and related results presented by Sano and Tachiya (3) for the steady state rate on a spherical surface are most easily obtained by direct integration of the diffusion equation, Eq. 25, which is described by Deutch (14). They are a straightforward generalization of the result of Kramers (12) and Debye (11) for diffusional systems where the dynamics occur in the radial direction. Note that for the spherical systems with a thin strip, the forms of the flux J^{ϵ}_{DV} and $J^{\epsilon}_{\text{BAR}}$ are the same.

RESULTS

In discussing our results we define $\gamma^2 r^2 = (2\lambda/D)\, r^2$ as the dimensionless parameter proportional to the flip-flop rate, λ, and the inverse of the diffusion coefficient, $1/D$. (We assume that the length in the planar model is equal to the radius r of the spherical model $l = r = 1\ \mu$m.). We define $J_{\text{Pmonolayer}}$ as the total flux for a planar monolayer; $J_{\text{Smonolayer}}$, the total flux for a spherical monolayer; J_{PO}, the total flux for a planar bilayer; J_{SO}, the total flux for a spherical bilayer; J_{PI}, the total flux for a planar bilayer with an impenetrable obstacle; J_{SI}, the total flux for a spherical bilayer with an impenetrable obstacle; J_{BPAR}, the total flux for a planar bilayer with a penetrable barrier.

In Figs. 2 and 3 we plot the ratio $(J_{\text{PO}}/J_{\text{Pmonolayer}})$ and $(J_{\text{SO}}/J_{\text{Smonolayer}})$ as a function of the log of $\gamma^2 r^2$. These curves show that for a bilayer without obstacle or barrier in the outer membrane, rapid flip-flopping will double the total rate by causing the two sides of the membrane to act like two parallel monolayers. These plots also suggest that there is a small difference between the behavior of the flux on planar and spherical surfaces: the results for the planar surface rise more sharply to the final value as a function of $\gamma^2 r^2$.

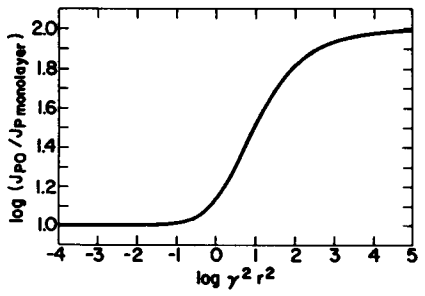

FIGURE 2 The log of the ratio of the total bilayer flux to the monolayer flux log ($J_{PO}/J_{P\ monolayer}$) is plotted vs. the log of $(2\lambda/D)\ r^2 = \gamma^2 r^2$ for a planar surface, where $r = 1\ \mu m$.

When there is an impenetrable obstacle in the outer membrane, flip-flopping must occur for the lipid probe to traverse the cell from apical to basolateral surfaces. Since diffusion is also taking place the rate of the slowest step will dominate. This behavior is shown in Figs. 4 or 5 where we plot the ratios (J_{P1}/J_{P0}) and (J_{S1}/J_{S0}) as a function of $\gamma^2 r^2$. Both curves are linear for very small $\gamma^2 r^2$ where the process is controlled by the rate of flip-flopping between inner and outer membrane. For $\gamma^2 r^2 \gg 1$, the rate of flip-flopping is so fast that the flux is independent of $\gamma^2 r^2$; the probes readily bypass the obstacle. In the transition region, $\gamma^2 r^2 \sim 1$, the time scales of the processes are comparable. The curves for the planar and spherical models (Figs. 4 and 5) are again almost identical.

A monolayer with a penetrable barrier displays similar behavior. In Fig. 6 we plot the ratio $(J_{PBAR}/J_{Pmonolayer})$ as a function of potential energy barrier height, ϕ, for a planar surface. We do not plot the corresponding result for a spherical surface because the curves differ only by factors independent of the barrier height. This last point can be seen by comparing Eqs. 22 and 23 and with Eqs. 30 and 28, respectively, if ϵ/l in Eqs. 22 and 23 is replaced by $Q_0(\epsilon)/Q_0(x_0)$, then the same curve will be generated. This curve (Fig. 6) is very similar in shape to the flip-flop cases (Figs. 4 and 5).

In Fig. 7 we have plotted the total rate (J_{P1}/c_0) as a function of the flip-flop rate, λ, for two diffusion coefficients. The chosen diffusion coefficients are approximately

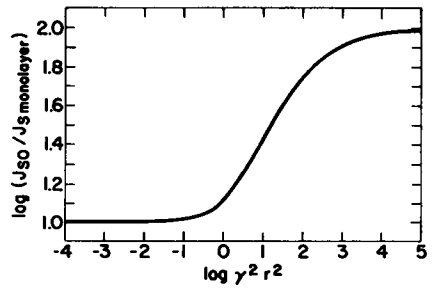

FIGURE 3 The log of the ratio of the total bilayer flux to the monolayer flux log ($J_{SO}/J_{S\ monolayer}$) is plotted vs. the log of $(2\lambda/D)\ r^2 = \gamma^2 r^2$, for a spherical surface where $r = 1\ \mu m$, $x_0 = \cos\theta_0 = 0.95$.

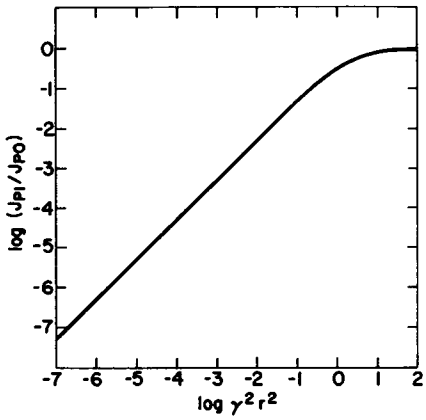

FIGURE 4 The log of the ratio of the total flux with an obstacle to the total flux in the absence of an obstacle log (J_{P1}/J_{P0}) is plotted vs. the log of $(2\lambda/D)\ r^2 = \gamma^2 r^2$ for a planar surface where $r = 1\ \mu m$.

equal to the largest and smallest diffusion coefficients measured by Dragsten et al. (4) and differ by an order of magnitude. As can be seen from Fig. 7, the total rates for the two different diffusion coefficients never differ by more than an order of magnitude. In fact for $\lambda < 10^{-2}\ s^{-1}$, the two curves corresponding to the different D's essentially coincide. It is only for $\lambda > 10^2\ s^{-1}$ that the two curves differ by close to an order of magnitude. The experimentally observed variations in flux between two probes with diffusion coefficients differing by a factor of three can only be explained, according to the model, if the flip-flop rates, λ, of the two probes are very different, at least by two orders of magnitude.

DISCUSSION

Given the experimental diffusion coefficients, the rates of flip-flopping between inner and outer membrane leaflets could be estimated theoretically if the rate of appearance of the lipid probe on the opposite side of the junction were measured. Dragsten et al. (4) observed only whether the

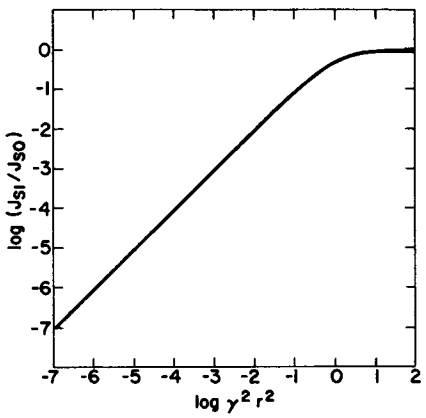

FIGURE 5 The log of the ratio of the total flux with an obstacle to the total flux in the absence of an obstacle log (J_{S1}/J_{SO}) is plotted vs. the log of $(2\lambda/D)\ r^2 = \gamma^2 r^2$ for a spherical surface where $r = 1\ \mu m$ and $x_0 = \cos\theta_0 = 0.95$.

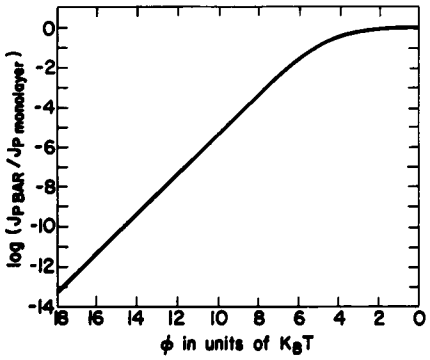

FIGURE 6 The log of the ratio of the flux with a barrier to the flux on a simple monolayer log ($J_{PBAR}/J_{P\,monolayer}$) is plotted vs. the potential energy barrier height, φ, for the planar surface where $\epsilon/l = 0.01$.

probe could move through the region of the tight junction to the side of the cell not labeled initially on the time scale of their experiment; no rates were explicitly reported. Our steady state calculation of the flux is a good estimate for this qualitative result. For a time-dependent experiment one generally expects a steady state approximation to give a good value for the rate of appearance of lipid probe at the sink at intermediate times of the experiment. From Fig. 3 *c* of Dragsten et al. (4) we observe that the time scale for appearance of AFC_{12} is hours; therefore the rate of appearance of the probe will be $\sim 10^{-4}$ to $10^{-3}\ s^{-1}$. From Fig. 7 we see that for the typical diffusion constants this rate can also be used as an estimate for the flip-flop rate. The absence of AFC_{16} on the opposite side suggests that its flip-flop rate is much smaller. From our calculation however, we see that this rate could just as well be the rate of crossing a penetrable barrier formed in the outer monolayer.

Note that the diffusion coefficient reported by Dragsten et al. (4) should be interpreted as an effective diffusion coefficient since the lipid probe can flip-flop to the inner membrane as well as diffuse in the outer membrane. When the probe can flip-flop between inner and outer leaflet of the membrane, the apparent diffusion coefficient will include contributions from probes that have flip-flopped to the inner leaflet, diffused, and then flip-flopped again to reappear in the outer leaflet. Figs. 2 and 3 show that for fast flip-flopping, i.e., large λ, the bilayer can act like two parallel monolayers and hence show a greater apparent diffusion coefficient.

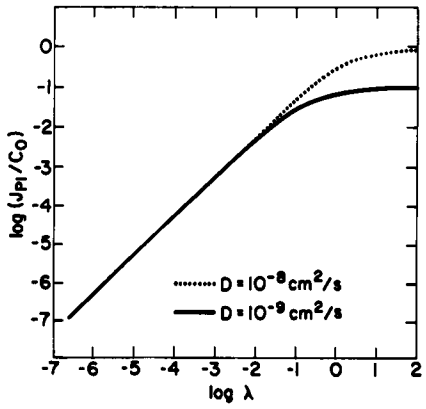

FIGURE 7 The log of the total rate for the planar surface log (J_{Pl}/C_0) is plotted vs. the log of the flip-flop rate, λ, for two different diffusion coefficients: $D = 10^{-8}\ cm^2/s$ and $D = 10^{-9}\ cm^2/s$.

This could be why Dragsten et al. (4) claim that the probes that were able to bypass the tight junction had diffusion coefficients between two to three times larger than those that could not. This does not change our conclusions in any way. Whether the two lipid probes have identical diffusion coefficients or diffusion coefficients differing by a factor of two or three, we find that the flip-flop rates must differ by at least an order of magnitude for the fluxes to differ by one order of magnitude in the linear regime of $\lambda < 10^{-2}\ s^{-1}$. Our rough estimate of the rates seems to indicate that this is in fact the experimental regime. If $\lambda > 10^{-2}\ s^{-1}$, the rates are independent of the flip-flop rates λ and will depend on how different the D's are.

In our results we found that the curves for the planar and spherical models were very similar in shape. This is true for the flip-flop models with an impenetrable barrier (Figs. 4 and 5) as well as for the penetrable barrier case (Fig. 6). This fact is very encouraging for future calculations of more sophisticated models, because it suggests that the simpler calculation on a planar surface gives as accurate qualitative results as does a much more tedious calculation on a spherical surface. It makes it possible to extend this work to cases where the protein-lipid concentration is different in the two halves of the cell and the distribution of the probe is not identical in both sides of the cell.

We find that two different models for the tight junction: (*a*) a penetrable barrier embedded in a monolayer, and (*b*) an impenetrable obstacle in the outer membrane of a bilayer that must be bypassed by flip-flopping between inner and outer membranes, give results for the flux that are very similar. If the flip-flop rate is an activated process $\lambda = Ae^{-\Delta\epsilon/K_BT}$, then it would be difficult to distinguish between the two models on the basis of the temperature dependence of the total flux.

APPENDIX A

In this Appendix we sketch the solution equation (Eq. 14) as obtained for the system equation (Eq. 12):

$$D\nabla^2 c_1^\alpha - \lambda(c_1^\alpha - c_2^\alpha) = 0$$
$$D\nabla^2 c_2^\alpha + \lambda(c_1^\alpha - c_2^\alpha) = 0, \qquad \text{(A1)}$$

where

$$\nabla^2 = \frac{1}{r^2 \sin\theta}\frac{\partial}{\partial\theta}\left(\sin\theta\frac{\partial}{\partial\theta}\right)$$

$$\alpha = + \quad \text{for} \quad \theta_0 < \theta < \pi/2$$

$$\alpha = - \quad \text{for} \quad \pi - \theta_0 > \theta > \pi/2.$$

Add the two equation in Eq. A1

$$D\nabla^2 (c_1^\alpha + c_2^\alpha) = 0. \quad \text{(A2)}$$

The solution of Eq. A2 is

$$c_1^\alpha + c_2^\alpha = f^\alpha P_0 + d^\alpha Q_0, \quad \text{(A3)}$$

which is substituted back into Eq. A1

$$\nabla^2 c_1^\alpha - \frac{2\lambda}{D} c_1^\alpha + \frac{\lambda}{D} [f^\alpha P_0 + d^\alpha Q_0] = 0. \quad \text{(A4)}$$

Define $\gamma^2 = 2\lambda/D$ and $\Delta = (\lambda/D)(f^\alpha P_0 + d^\alpha Q_0)$, then Eq. A4 becomes $\nabla^2 c_1^\alpha - \gamma^2 c_1^\alpha + \Delta = 0$. With the substitution $c_1^\alpha = C_1^\alpha + \Delta/\gamma^2$, Eq. A4 becomes

$$\nabla^2 C_1^\alpha - \gamma^2 C_1^\alpha = 0 \quad \text{(A5)}$$

with the following solution

$$C_1^\alpha = a^\alpha P_\nu(x) + b^\alpha Q_\nu(x), \quad \text{(A6)}$$

so that

$$c_1^\alpha = a^\alpha P_\nu(x) + b^\alpha Q_\nu(x) + \frac{\Delta}{\gamma^2}$$

$$c_2^\alpha = f^\alpha P_0 + d^\alpha Q_0 - a^\alpha P_\nu(x) - b^\alpha Q_\nu(x) - \frac{\Delta}{\gamma^2}. \quad \text{(A7)}$$

For $\theta_0 < \theta < \pi/2$

$$c_1^+ = a^+ P_\nu(x) + b^+ Q_\nu(x) + \tfrac{1}{2}[f^+ P_0 + d^+ Q_0]$$

$$c_2^+ = a^+ P_\nu(x) - b^+ Q_\nu(x) + \tfrac{1}{2}[f^+ P_0 + d^+ Q_0]. \quad \text{(A8)}$$

For $\pi - \theta_0 > \theta > \pi/2$

$$c_1^- = a^- P_\nu(x) + b^- Q_\nu(x) + \tfrac{1}{2}[f^- P_0 + d^- Q_0]$$

$$c_2^- = -a^- P_\nu(x) - b^- Q_\nu(x) + \tfrac{1}{2}[f^- P_0 + d^- Q_0]. \quad \text{(A9)}$$

When we apply the eight boundary conditions (Eqs. 2–9) where l is replaced by $\cos\theta_0 = x_0$ and $x = \cos\theta$, we obtain the following set of eight equations with eight unknowns $(a^+, b^+, f^+, d^+, a^-, b^-, f^-, d^-)$

$$c_0 = a^- P_\nu(-x_0) + b^- Q_\nu(-x_0) + \frac{1}{2}[f^- + d^- Q_0(-x_0)] \quad \text{(A10)}$$

$$0 = a^+ P_\nu(x_0) + b^+ Q_\nu(x_0) + \frac{1}{2}[f^+ + d^+ Q_0(x_0)] \quad \text{(A11)}$$

$$0 = -a^+ P'_\nu(x_0) - b^+ Q'_\nu(x_0) + \frac{1}{2} d^+ Q'_0(x_0) \quad \text{(A12)}$$

$$0 = -a^- P'_\nu(-x_0) - b^- Q'_\nu(-x_0) + \frac{1}{2} d^- Q'_0(-x_0) \quad \text{(A13)}$$

$$0 = a^+ P'_\nu(0) + b^+ Q'_\nu(0) + \frac{1}{2} d^+ \quad \text{(A14)}$$

$$0 = a^- P'_\nu(0) + b^- Q'_\nu(0) + \frac{1}{2} d^- \quad \text{(A15)}$$

$$-a^+ P_\nu(0) - b^+ Q_\nu(0) + \frac{1}{2} f^+ = -a^- P_\nu(0) - b^- Q_\nu(0) + \frac{1}{2} f^- \quad \text{(A16)}$$

$$-a^+ P'_\nu(0) - b^+ Q'_\nu(0) + \frac{1}{2} d^+ = -a^- P'_\nu(0) - b^- Q'_\nu(0) + \frac{1}{2} d^-, \quad \text{(A17)}$$

where $P_0 = 1$, primes denote differentiation with respect to x, and $Q_0(x) = 1/2 \ln[(1 + x)/(1 - x)]$ so that $Q'_0(0) = 1$ and $Q_0(0) = 0$. This system of equations is solved and

$$J_{S1} = D \left.\frac{\partial c_2}{\partial x}\right|_{x=0} = d^\alpha. \quad \text{(A18)}$$

We thank Robert L. Fulton for helpful discussions.

Supported in part by the Defense Advanced Research Projects Agency and the National Science Foundation.

Received for publication 15 December 1982 and in revised form 6 May 1983.

REFERENCES

1. Edidin, M. 1974. Rotational and translational diffusion in membranes. *Annu. Rev. Biophys. Bioeng.* 3:179–201.
2. Aizenbud, B. M., and N. D. Gershon. 1982. Diffusion of molecules on biological membranes of nonplanar form. A theoretical study. *Biophys. J.* 38:287–293.
3. Sano, H., and M. Tachiya. 1981. Theory of diffusion controlled reactions on spherical surfaces and its application to reactions on micellar surfaces. *J. Chem. Phys.* 75:2870–2878.
4. Dragsten, P. R., R. Blumenthal, and J. S. Handler. 1981. Membrane assymetry in epithelia: is the tight junction a barrier to diffusion in the plasma membrane? *Nature (Lond.).* 294:718–722.
5. Kachar, B., and T. S. Reese. 1982. Evidence for the lipidic nature of tight junction strands. *Nature (Lond.).* 296:464–466.
6. Galli, P., A. Brenna, P. deCamilli, and J. Meldolesi. 1976. Extracellular calcium and the organization of tight junctions in pancreatic acinar cells. *Exp. Cell. Res.* 99:178–183.
7. Hoi Sang, Ü., M. H. Saier, and M. H. Ellisman. 1979. Tight junction formation is closely linked to the polar redistribution of intramembraneous particles in aggregating MDCK epithelia. *Exp. Cell Res.* 122:384–391.
8. Meldolesi, J., G. Castiglioni, R. Parma, N. Nassivera, and P. deCamilli. 1978. Ca^{++}-dependent disassembly and reassembly of occluding junctions in guinea pig pancreatic acinar cells. *J. Cell Biol.* 79:156–172.
9. Pissam, M., and P. Ripoche. 1976. Redistribution of surface macromolecules in dissociated epithelial cells. *J. Cell Biol.* 71:907–920.
10. Cereijido, M., J. Ehrenfeld, I. Meza, and A. Martinez-Palomo. 1980. Structural and functional membrane polarity in cultured monolayers of MDCK cells. *J. Membr. Biol.* 52:147–159.
11. Debye, P. 1929. Polar Molecules. Chemical Catalog Company, Inc., New York. 77–108.
12. Kramers, H. A. 1940. Brownian motion in a field of force and the diffusion model of chemical reactions. *Physica (Utrecht).* 7:284–304.
13. Abramowitz, M., and I. Stegun. 1972. Handbook of Mathematical Functions. Dover Publications, Inc., New York. 332–341.
14. Deutch, J. M. 1980. A simple method for determining the mean passage time for diffusion controlled processes. *J. Chem. Phys.* 73:4700–4701.
15. Lebedev, N. N. 1972. Special Functions and Their Applications. R. A. Silverman, editor. Dover Publications, Inc., New York. 189–199.